Asian Journal of Chemistry Vol. 22, No. 5 (2010), 3458-3468

Effects of Inorganic Mercury on the Conformation and Activity of Glutathione S-transferase from *Schistosoma japonicum*

XIN-HE HUANG, YU HUANG, HAI-LIANG GAO, JUN-XI YAN and LIN-FANG DU*
Key Laboratory of Bio-resources and Eco-environment of the Ministry of Education, College of Life Sciences, Institute of Nanobiomedical Technology and Membrane Biology, Sichuan University, Chengdu 610064, P.R. China
Fax: (86)(28)85415300; E-mail: dulinfang@yahoo.com

Glutathione S-transferases (GST) are a family of cytosolic or membrane-bound multifunctional enzymes present in all organisms with their main function in the detoxification of harmful physiological and xenobiotic compounds. To study the interaction between GST and toxic heavy metal ion (Hg^{2+}), the 26 kD glutathione S-transferase from *Schistosoma japonicum* (Sj26GST) was expressed in *Escherichia coli* and purified by glutathione-sepharose affinity chromatography. The effects of Hg^{2+} ion on the conformation and activity of Sj26GST were studied by spectrum method and enzymatic kinetics determination, respectively. Binding of Hg^{2+} ion to Sj26GST produced a UV difference absorbance peak that is characteristic of ligand-to-metal charge transition (LMCT) bands and quantitative analysis indicates Sj26GST has two categories of Hg^{2+} ion binding sites at least. Gradual quenching of Sj26GST intrinsic fluorescence induced by Hg^{2+} ion was observed at the excitation wavelength of 295 nm and the quenching was of static-quenching with a quenching constant of 3.39×10^{11} mol/L^{-1} s^{-1}. Far-UV and near-UV CD spectra showed that incubation of Sj26GST with Hg^{2+} ion resulted in slight conformational changes in either secondary or tertiary structure of Sj26GST, exhibiting a minor decrease in α-helix content and a slight increase in content of unordered coil. Enzyme activity and kinetic studies indicated Hg^{2+} ion inhibited Sj26GST activity in a non-competitive form. Generally speaking, the spectral data and kinetic constants indicated that the binding of Hg^{2+} ion induced Sj26GST to undergo a microstructural change that appears to impact on the functional conformation of the active site.

Key Words: Glutathione S-transferase, Inorganic mercury, Inhibition, Ultraviolet difference, Fluorescence, Circular dichroism.

INTRODUCTION

Mercury is a non-essential element. However, trace mercury is highly toxic for organisms[1]. Mercury residues from gold mining, agriculture, industries and hospitals have been dispersed indiscriminately, sometimes resulting in several thousand-fold increases in mercury basal levels[2,3]. Mercury can be readily absorbed through respiratory and gastrointestinal tract or through unbroken skin. Mercury bioaccumulation

derived from human intervention puts at risk the native fauna, flora and microflora and represents a strong environmental hazard[4,5]. Mercury removal is a challenge for environmental improvement. Commonly used mercury removal processes, such as those based on ion exchange, have been sensitive to environmental conditions[6], so these methods may fail to remove or recover the toxic metal ions.

Knowledge of detoxification mechanisms may facilitate the development of a possible biotransformation process to eliminate mercury ion in nature. The detoxifying enzymes which are involved in the glutathione dependent enzymes, glutathione S-transferases and glutathione peroxidase[7]. Glutathione S-transferases (GSTs, EC 2.5.1.18) are a family of dimeric multifunctional proteins, which play a crucial role in the biotransformation of potentially toxic xenobiotics[8]; other functions, not associated with detoxification, include repair of macromolecules oxidized by reactive oxygen species, regeneration of S-thiolated proteins, biosynthesis of physiologically important metabolites and impact of signaling kinases[9,10]. Glutathione S-transferases catalyze the combination of reduced glutathione (GSH, γ-Glu-Cys-Gly) to a variety of physiological and xenobiotic electrophiles by conjugating the electrophilic centers to the sulfur atom of GSH and the resultant water-soluble S-conjugate is processed and eliminated *via* the mercapturate pathway[11,12]. Glutathione S-transferases have been previously demonstrated to detoxify such electrophiles as alachlor, atrazine, DDT, lindane and methyl parathion *via* GST conjugation[13]. There is report on the inhibition of the activity of the *Boophilus microplus* recombinant glutathione S-transfease by several acaricides (*e.g.*, ethion, amitraz, chlorpyrifos, cypermethrin, diazinon, ivermectin, deltamethrin and flumethrin)[14] and the resistance to organochlorine and organophosphate insecticides is specifically associated with increased GST activity[15]. However, the studies on the inhibition of glutathione S-transferase by free toxic metal ions are inadequate. Previously, Cursino *et al.*[16] reported that genetically engineered *Escherichia coli* strains expressing glutathione S-transferase (Sm28GST from *Schistosoma mansoni*) demonstrated mercury chloride resistance, but there are no definitive structural data available at present concerning the exact location and specific property of the non-substrate-binding sites on the enzyme. When GSTs function as their ligand-binding or ligand in, catalytic activity was usually inhibited in a non-competitive manner[17]. However, the conformational basis of the catalytic function is modulated by the occupation of these sites is limited. Meanwhile, GSTs *in vivo* have become significant therapeutic targets in certain diseases and has been shown to be over expressed in a broad spectrum of tumor cells[18]; especially *Schistosoma japonicum* GSTs, the major detoxification enzymes in *Schistosoma japonicum*, have promising vaccine potential against *Schistosomiasis* and their inhibitors are novel antischistosomal drugs[19].

In the present work, the 26 kDa GST from *Schistosoma japonicum* (Sj26GST) was expressed and purified. The binding properties of purified Sj26GST with Hg^{2+} ion were studied by spectroscopic methods and the subsequent conformational changes and the enzyme activity were assayed. Results of this study is of great

value in understanding the mechanism of Sj26GST detoxification and may provide novel perspectives in developing an improved bioremediation alternative to remove and recover poisonous heavy metal from and in contaminated environment.

EXPERIMENTAL

Bacterial strains, vectors, enzymes and reagents: *E. coli* BL21(DE3) were preserved in this laboratory. The plasmid used was pGEX-5X-3 containing 26 kDa glutathione S-transferase gene from *Schistosoma japonicum*, which was supplied by Amersham Biosciences. Glutathione sepharose 4 fast flow affinity column were supplied by Amersham Bioscience (USA). Peroxidase-conjugated goat anti-mouse IgG secondary antibody was provided by Bio-Rad (USA). IPTG, ampicillin and reduced glutathione were from Amresco (USA). Mercury chloride, 1-chloro-2,4-dinitrobenzene (CDNB), DTT, PMSF and reduced glutathione (GSH) were purchased from Sigma (USA). All other reagents were of research grade or better and were obtained from commercial sources.

Expression and purification of Sj26GST: The expression plasmid above was transformed into *E. coli* BL21 (DE3) competent cell, a single colony of *E. coli* BL21 (DE3) harboring the pGEX-5X-3 plasmid was incubated overnight at 37 ºC in Luria-Bertani (LB) culture medium containing 100 μg/mL of ampicillin. The culture was diluted 50 times in fresh LB culture medium with 100 μg/mL of ampicillin and grown at 37 ºC until the absorbance at 600 nm reached 0.6, then isopropyl-β-D-thiogalactopyranoside (IPTG) was added at a final concentration of 1.0 mmol/L and incubation was continued for another 3 h at 29 ºC, afterwards the bacterial cells were harvested by centrifugation and the bacterial pellets were resuspended in phosphate-buffered saline (PBS) containing 1 mmol/L PMSF, 1 mmol/L DTT, 5 mmol/L EDTA and then sonicated on ice in short burst. Triton-X-100 (1 % final concentration) was added and the solution was gently stirred at 4 ºC for 1 h to facilitate solubilization of proteins. The supernate was then collected by centrifugation and it was applied directly onto a glutathione affinity chromatography column. After the Sj26GST protein was bound to the matrix, the column was washed with PBS containing 0.5 mol/L NaCl to remove non-specifically bound protein. Sj26GST was eluted with 10 mmol/L reduced glutathione. The purity of the enzyme was detected by sodium dodecyl sulfate-polyacrylamide gel electrophoresis (SDS-PAGE).

Inhibition of Sj26GST induced by Hg^{2+} ion and Sj26GST activity assay: The Sj26GST activity was measured on a Shimadzu UV-240 spectrophotometer at 25 ºC using CDNB and GSH as substrates by the Habig-Jakoby methods[8]. The dynamic formation of dinitrophenyl thioether was monitored at 340 nm and the linear progressive curves were corrected for the corresponding nonenzymatic controls. Protein concentrations were determined from absorbance measurement at 280 nm using a molar extinction coefficient of 3.03×10^4 mol/L^{-1} cm^{-1} for enzyme monomer, as calculated by the Gill-von Hippel method[20].

Mercury chloride solution was prepared freshly in 0.1 mol/L phosphate buffer at pH 6.5. For inhibition assay, Hg^{2+} ion in different concentration was mixed with Sj26GST and the solution was incubated at 25 ºC for 2 min. The reaction was initiated by the addition of 1 mmol/L CDNB and 1 mmol/L GSH. The formation of S-(2,4-dinitrophenyl)-glutathione was monitored at 340 nm. Thus, apparent inhibition constant for Hg^{2+} ion and the inhibition type induced by Hg^{2+} ion, using CDNB as co-substrate, were determined at fixed concentration of GSH and at different concentrations of non-substrate Hg^{2+} ion ligand.

Measurement of UV difference spectra: UV difference spectra were recorded on a Shimadzu UV-240 spectrophotometer with wavelengths ranging from 190 nm to 300 nm at 25 ºC. The purified Sj26GST in 0.1 mol/L phosphate buffer at pH 6.5 was titrated with a series of concentrations Hg^{2+} ion solution prepared in the same buffer. The purified Sj26GST of the same concentration without Hg^{2+} ion was used as the reference. The UV difference spectra were performed at intervals of 2 min after the addition of Hg^{2+} ion.

Measurement of fluorescence spectra: Fluorescence emission spectra were measured at 25 ºC on a Hitachi F-4500 fluorescence spectrophotometer. Intrinsic fluorescence of Sj26GST was measured by recording the emission spectra in the range of 310-450 nm at an excitation wavelength of 295 nm to selectively excite tryptophans. Excitation bandwidth was 2.5 nm and emission bandwidth was 5 nm. Spectra were recorded 2 min after the addition of Hg^{2+} ion. The solvent spectrum obtained under the same conditions was subtracted to obtain the actual sample spectrum. Each single outcome was expressed as the calculated mean of three separate scans. The quenching constants were obtained from Stern-Volmer equation and plots[21,22].

Measurement of CD spectra: CD spectra measurements were performed at 25 ºC with an AVIV Model 400 spectrophotometer. The path length of the cell used was 2 mm for the far-UV CD spectra and 1 cm for the near-UV CD spectra. Both far-UV and near-UV CD spectra were recorded 2 min after the addition of Hg^{2+} ion and were expressed as molar CD, $\Delta\varepsilon$ (mol L^{-1} cm^{-1}). The solvent spectrum obtained under the same conditions was subtracted to obtain the actual sample spectrum. Each single outcome was expressed as the calculated mean of three separate scans.

RESULTS AND DISCUSSION

Hg^{2+} ion induced inhibition of Sj26GST activity: Sj26GST was expressed in *E. coli* BL21 (DE3), which had been transformed with the pGEX-5X-3 plasmid and purified by Glutathione-Sepharose affinity chromatography column. SDS-PAGE analysis indicated the purified Sj26GST was obtained as a pure preparation (Fig. 1).

Effects of Hg^{2+} ion on the activity of Sj26GST was investigated spectrophotometrically by measuring the dynamic formation of dinitrophenyl thioether at 340 nm. Fig. 2A indicated the dependence of percentage inhibition on Hg^{2+} ion concentration, the slope of the inhibition plot is increasing gradually and the tendency of

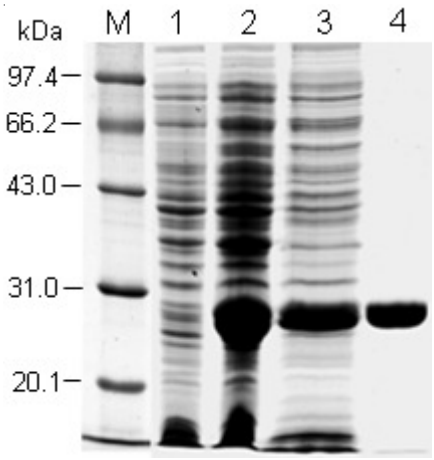

Fig. 1. Purification of Sj26GST. M: protein marker; 1, 2: BL21 (DE3) with pGEX-5X-3 plasmid without induction and induction; 3: the soluble expression of Sj26GST; 4: the purified Sj26GST

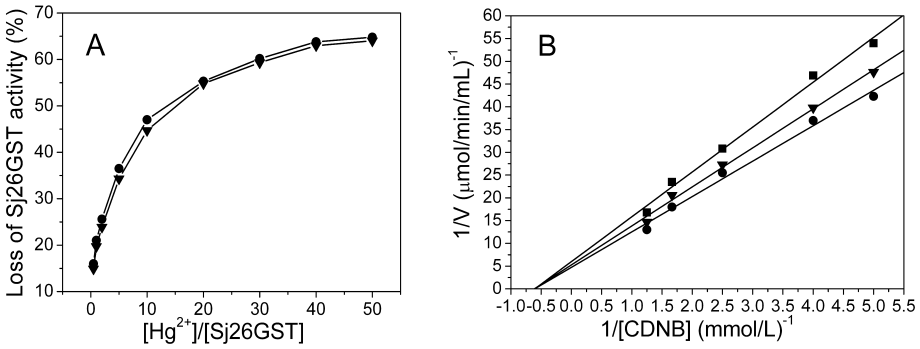

Fig. 2. Dependence of the percentage of inhibition (A) and the steady-state kinetics (B) of Sj26GST with or without Hg^{2+} ion. The activity of the enzyme was measured in 0.1 mol/L phosphate buffer at pH 6.5. A: The concentration of CDNB is 0.4 (▼) and 0.6 mmol/L (●), respectively. B: The straight line plots of (initial rate)-1 versus (CDNB)-1 refer to Hg2+ ion concentration of 0 (●), 50 (▼), 100 (■) μmol/L from bottom to top

inhibition is obvious. The inhibition scheme at two different CDNB concentrations showed similar behaviours of inhibition, which is one of the characters of non-competitive inhibition. The Lineweaver-Burk (LB) double reciprocal plot gave the value of Michaelis constant (K_m) as 1.64 mmol/L to co-substrate CDNB. Weather Since substrate GSH The LB plot of the steady-state kinetics with varying Hg^{2+} ion concentration gave straight lines that meet at a single point on the horizontal axis (Fig. 2B). This type of inhibition has been termed as linear non-competitive inhibition, which is consistent with the conclusion above and this result suggested that the presence of Hg^{2+} ion did not affect the binding of CDNB to the enzyme and Hg^{2+}

ion shares different binding sites to the enzyme with CDNB. Mechanistically this type of inhibition allows change in the maximum velocity (V_{max}) while keeping K_m unaltered.

Ligand-metal charge transition bands and conformational transition of Sj26GST induced by binding of Hg^{2+} ion: When metal ions interact with protein, the charge transitions from the ligand on protein to the metal ions can be detected in the UV wavelength region[23]. The ligand-to-metal charge transition (LMCT) band is an effective tool to study the interaction between metal ions and protein[23]. The addition of series of aliquots of Hg^{2+} ion into the solution containing 5 μmol/L Sj26GST in 0.1 mol/L phosphate buffer at pH 6.5, produced UV difference spectra as shown in Fig. 3A. A salient absorbance peak of LMCT bands was detected and the absorption intensity increased dramatically and the maximum absorption wavelength (λ_{max}) was shifted from 215 to 230 nm as the ratio of [Hg^{2+}]/[E] increased from 5 to 40.

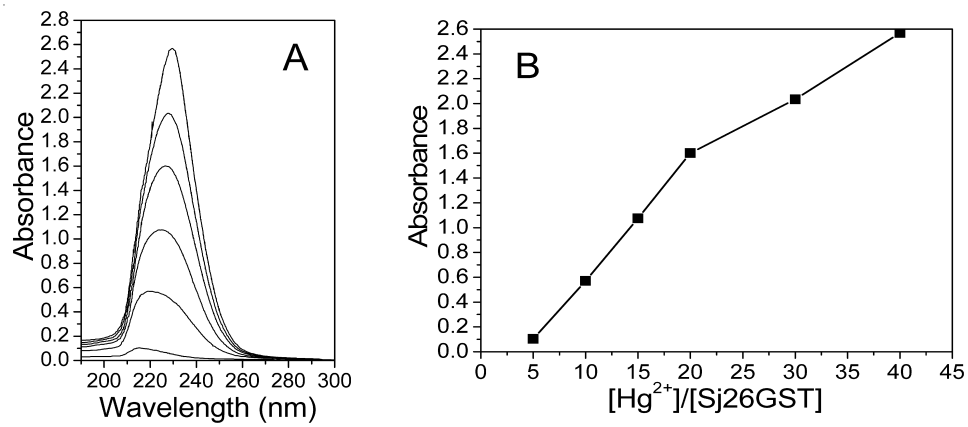

Fig. 3. UV difference spectra (A) and Titration curve (B) of Sj26GST for the addition of Hg^{2+} ion. The concentration of Sj26GST is 5 μmol/L in 0.1 mol/L phosphate buffer at pH 6.5. A: The concentrations of Hg^{2+} ion are 5, 25, 50, 100, 150 and 200 μmol/L from bottom to top

For further study of the details of Hg^{2+} ion binding with Sj26GST, we got the plot of absorbance values at peak in LMCT bands *versus* the ratio of concentration of Hg^{2+} ion to Sj26GST. As shown in Fig. 3B, the curve had an inflexion when the ratio of [Hg^{2+}]/[E] arrives at 20, suggesting that Sj26GST protein contains two kinds of binding sites, of which one is prone to be saturated with high affinity to Hg^{2+} ion and the other has higher capacity of accommodating Hg^{2+} ion with lower affinity.

Mercury(II) ion is considered to be a soft ion and soft Lewis acids, which presents an exceptional affinity for sulfhydryls group of proteins[24]. Crystallographic data indicate that each subunit of Sj26GST contains four cysteine residues (Cys85, Cys138, Cys169 and Cys178), with only the Cys169 residue buries inside the molecule

and the other three locate on the surface of the protein and are highly exposed to solvent[19,25]. Neither intra- nor inter-disulfide linkage exists in the active dimeric enzyme of the recombinant Sj26GST[19,25]. Therefore, it can be presumed that the three superficial Cys residues integrate easily with Hg^{2+} ion in a hydrophobic binding form at a low metal ion concentration and due to the binding of Hg^{2+} ion with the superficial Cys residues, Sj26GST undergoes a conformational transition from the original conformation in the absence of Hg^{2+} ion to the conformation binding with Hg^{2+} ion and this conformational transition probably enhances the binding of Hg^{2+} ion and promotes the formation of Hg^{2+} ion centers in protein. As a result, gradual increase of absorbance values at peak in LMCT bands was observed, at the same time the conformational transition of Sj26GST leads to a more polar microenvironment of the aromatic amino acids in Sj26GST, especially the polarity of the tyrosine, which is well conserved and critical for enzymatic catalytic activity, so a red shift of LMCT bands was observed. When the ratio of $[Hg^{2+}]/[E]$ reached to 20, the three superficial cysteine residues were saturated, which leads to the less dramatic red-shift and enhancement at peak in LMCT bands and the less inhibition of enzyme activity.

Quenching of fluorescence of Sj26GST induced by Hg^{2+} ion: The fluorescence spectra of Sj26GST, similar to those of most proteins, are dominated by emission from tryptophane residues and the fluorescence can be quenched when a cation, such as a transition metal ion or lanthanide ion is bound nearby[21,22]. Fluorescence quenching has been widely utilized as a powerful means to investigate the accessibility of fluorophores in the protein matrix to quenchers[22]. Each subunit of Sj26GST contains four tryptophane residues at positions 8, 41, 201 and 206[19,25], which can be used as fluorescence reporter groups for studying protein conformation. Fig. 4A illustrated the fluorescence quenching of Sj26GST induced by Hg^{2+} ion. It can be seen that the quenching without remarkable red or blue shift was achieved when the Hg^{2+} ion concentration increased. One estimate concerning the reason might be that the hydrophobic microenvironment of the tryptophane residues became more exposed to solvent and the energy can be transferred from tryptophane to Hg^{2+} ion, so metal binding is thus accompanied by a substantial decrease in Sj26GST fluorescence. It seems quite reasonable to expect that the four tryptophane residues in Sj26GST have different accessibility to Hg^{2+} ion, with at least one located in a more hydrophobic environment and thus less accessible to Hg^{2+} ion. May be the less accessible Trp is Trp8, which is placed next to Tyr7 that is implied at the substrate binding at the active site of the enzyme and the less accessibility of Trp8 accounted for partly that the binding of Hg^{2+} ion did not inhibit the activity of Sj26GST completely.

As mentioned above, fluorescence quenching measurement can also be used to monitor metal binding and there are two major quenching processes *i.e.*, static and dynamic quenching. Both of which are involved in the molecular contact between the fluorophore and the quencher. Static quenching refers to the formation of a non-fluorescent fluorophore-quencher complex, namely ground-state complex. Dynamic quenching, a collisional process, refers to the quencher diffusion to the

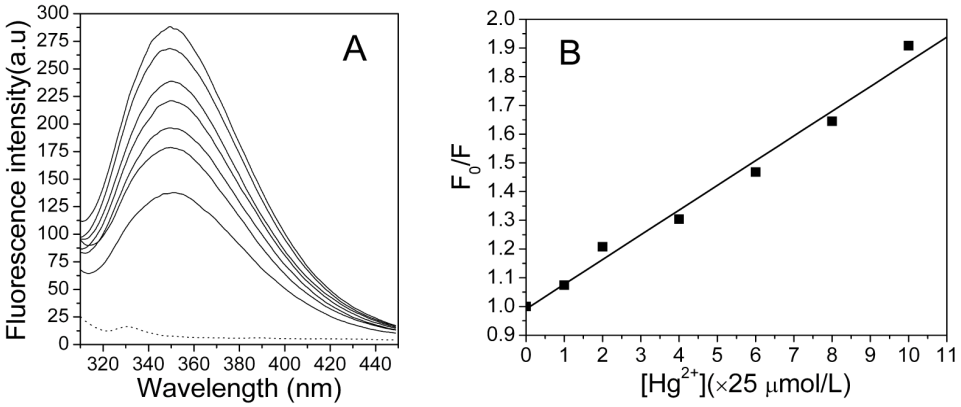

Fig. 4. Quenching of fluorescence of Sj26GST protein induced by Hg^{2+} (A) and plot of F_0/F *vs.* $[Hg^{2+}]$ (B). A: The Sj26GST protein concentration is 5 μmol/L in 0.1 mol/L phosphate buffer at pH 6.5. Hg^{2+} concentration is 0, 25, 50, 100, 150 and 200 μmol/L from the top solid line to the bottom, respectively. The excitation wavelength is 295 nm

fluorophore during the lifetime of the excited state and upon contact, the fluorophore returns to the ground state without emitting photons. Both static and dynamic processes can be characterized by the Stern-Volmer equation[21,22]:

$$F_0/F = 1 + K_{SV}[Q] = 1 + K_q\tau_0[Q]$$

where F_0 or F are the fluorescence intensity of the Sj26GST in the absence or presence of different concentration of Hg^{2+} ion, [Q] is the concentration of the quencher and K_{SV} is the Stern-Volmer quenching constant which can be written as $K_{SV} = K_q\tau_0$, where K_q is the bimolecular quenching constant, τ_0 is the lifetime of the fluorophore in the absence of quencher and is 10 ns for biological macromolecules. Then K_q can be calculated from K_{SV} obtained from the slope of Stern-Volmer plot. Data of Fig. 4A were analyzed by Stern-Volmer equation above, as shown in Fig. 4B, for Hg^{2+} ion, the K_q is 3.39×10^{11} mol L^{-1} s^{-1}, which is much higher than the biomolecular quenching constant (2.0×10^{10} mol L^{-1} s^{-1}) of other quenchers. Accordingly, the quenching of Sj26GST induced by Hg^{2+} ion is probably static-quenching, which implies that a nonfluorescent complex of protein-metal ion was formed during the binding of Hg^{2+} ion and Sj26GST.

CD spectra of Sj26GST in the absence and presence of Hg^{2+} ion: CD spectra are a sensitive physical technique for determining structure and monitoring structural changes of biomolecules. The far-UV CD spectra of proteins are highly sensitive toward protein structure, thus especially helpful for determining the changes of protein secondary structure[26]. To study the effect of Hg^{2+} ion on the secondary structure of Sj26GST, we measured the far-UV CD spectra of Sj26GST induced by various concentration Hg^{2+} ion. As can be seen from Fig. 5A, the far-UV CD spectra of Sj26GST in the absence of Hg^{2+} ion exhibited a weak negative peak at 208 nm, a typical character of the α-helix structure and a broad and strong negative peak in

the range of 220-230 nm, which is also characteristic of the α-helix structure but obscured by other second structure, such as β-sheet or unordered coil. When incubated with Hg^{2+} ion, the far-UV CD spectra of Sj26GST had no apparent changes, revealing a similar spectrum to that of native spectrum.

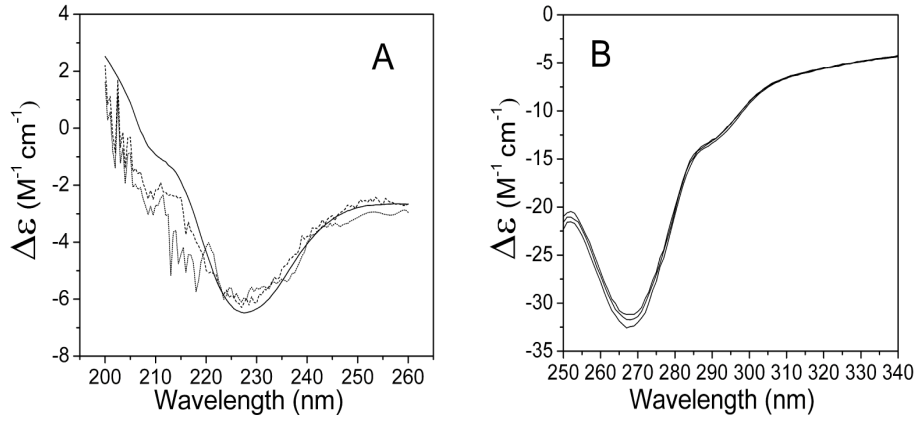

Fig. 5. Far-UV (A) and near-UV (B) circular dichroism spectra of Sj26GST protein. A: The protein concentration is 10 μmol/L in 0.1 mol/L phosphate buffer at pH 6.5. Solid line, dash line and dot line refer to Sj26GST protein without Hg^{2+} ion, with 50 μmol/L and 100 μmol/L Hg^{2+} ion, respectively. B: The protein concentration is 50 μmol/L in 0.1 mol/L phosphate buffer at pH 6.5. Solid lines from bottom to top refer to Sj26GST protein without Hg^{2+} ion, with 250 and 500 μmol/L Hg^{2+} ion, respectively

Furthermore, quantitative analysis of the content of secondary structure of Sj26GST with or without Hg^{2+} ion applying CD pro software was shown in Table-1. From the table, it can be seen that Sj26GST was dominated by α-helix structure, which was consistent with previous reports[19,25]. Table-1 also showed the adding of Hg^{2+} ion resulted in slight conformational change in the content of secondary structure, exhibiting a minor decrease of α-helix and a slight increase in unordered coil; these results agree well with the outcome shown in Fig. 5A.

TABLE-1
CONTENT OF SECONDARY STRUCTURE OF SJ26GST
CALCULATED BY CD PRO SOFTWARE

	H(r)	H(d)	S(r)	S(d)	T	U
Sj26GST	23.2	22.9	11.5	14.8	18.6	9.0
Sj26GST treated by 50 μmol/L Hg^{2+} ion	22.0	21.9	10.4	15.0	18.9	12.8
Sj26GST treated by 100 μmol/L Hg^{2+} ion	20.0	22.6	10.0	13.6	19.0	14.8

Note: (1) The figures in the table are percentage content; (2) H(r), H (d), S(r), S (d), T, U stand for regular helix, distorted helix, regular sheet, distorted sheet, turn and unordered coil, respectively.

The near-UV CD spectra of proteins reflect contributions of aromatic side chains and disulfide bonds to the conformation of proteins[26]. The CD spectra in the 260-300 nm region are used for monitoring the environmental changes of tyrosine and tryptophane residues in the globin; changes at the 290-300 nm region are ascribable to local environment alteration of tryptophane residues and CD bands in the 260-290 nm are characteristic of tyrosine residues but obscured by those of tryptophane residues[26]. As shown in Fig. 5B, the near-UV CD spectrum of Sj26GST in the absence or presence of Hg^{2+} ion showed that the adding of Hg^{2+} ion led to a minor change of negative peaks at both 268 and 292 nm. These results indicated that Hg^{2+} ion binding brought slight local microenvironment alteration of both tyrosine and tryptophane residues located, reflecting a less-ordered tertiary structure.

Conclusion

In the present work the effects of Hg^{2+} ion on the conformation and activity of the purified Sj26GST were investigated by spectrum methods and enzymatic kinetics assay. Results showed Hg^{2+} ion bond to purified Sj26GST with high affinity in the hydrophobic form mainly through the three superficial cysteine residues (Cys85, Cys138 and Cys178) of protein and inhibited Sj26GST activity tenderly in a non-competitive form; both fluorescence and CD spectra of Sj26GST in the absence and presence of Hg^{2+} ion indicated the conformation of Sj26GST, such as the tryptophane intrinsic fluorescence, the secondary and tertiary structure of Sj26GST, can not be significantly effected by Hg^{2+} ion, therefore it is assumed that the binding of Hg^{2+} ion to Sj26GST might be accompanied by other interactions, whose contribution is being remained to be further studied. Taken together, the binding properties of Sj26GST with Hg^{2+} ion indicate that the Sj26GST protein has a high affinity and capacity of accommodating Hg^{2+} ion. These data suggest that Sj26GST may act as an antidotal protein to sequester heavy metal, such as Hg^{2+} ion and it seems quite reasonable to expect that those recombinant cells containing the gene of Sj26GST may, in the near future, be utilized as a means of bioremediation to remove or recover inorganic mercury from contaminated effluents, industry effluent, for instance.

ACKNOWLEDGEMENTS

This work is supported by the Ministry of Education of China for Excellent Youth Teacher Foundation (NCET-04-0861) and Sichuan University Research Grant 985.

REFERENCES

1. D.Z. Gao, J.J. Wang and J.L. Cai, *J. Environ. Sci.*, **3**, 105 (1991).
2. A.O. Summers, *Ann. Rev. Microbiol.*, **40**, 607 (1986).
3. T. Barkay, R. Turner, E. Saouter and J. Horn, *Biodegradation*, **3**, 147 (1992).
4. J.B. Robinson and O.H. Tuovinen, *Microbiol. Res.*, **48**, 95 (1984).
5. T. Barkay, *Appl. Environ. Microbiol.*, **53**, 2725 (1987).
6. J.A. Ritter and J.P. Bibler, *Water Sci. Technol.*, **25**, 165 (1992).

7. Y. Ding, J.L. Miao, G.Y. Li, Q.F. Wang, G.F. Kan and G.D. Wang, *J. Environ. Sci.*, **17**, 667 (2005).
8. W.H. Habig and W.B. Jakoby, *Method Enzymol.*, **77**, 398 (1981).
9. R.N. Armstrong, *Chem. Res. Toxicol.*, **10**, 2 (1997).
10. D. Sheehan, G. Meade, V.M. Foley and C.A. Down, *Biochem. J.*, **360**, 1 (2001).
11. Y. Takahashi, E.A. Campbell, Y. Hirata, T. Takayama and I. Listowsky, *J. Biol. Chem.*, **268**, 8893 (1993).
12. A. Nepoiv, R. Podlipna, P. Soudek, P. Schroder and T. Vanek, *Chemosphere*, **57**, 1007 (2004).
13. J.D. Hayes and D.J. Pulford, *Crit. Rev. Biochem. Mol. Biol.*, **30**, 445 (1995).
14. I.J. da Silva Vaz, T.T. Lermen, A. Michelon, C.A.S. Ferreira, D.R. Joaquim de Freitas, C. Termignoni and A. Masuda, *Vet. Parasitol.*, **119**, 237 (2004).
15. J.G. Vontas, A.A. Enayati, G.J. Small and J. Hemingway, *Pestic. Biochem. Physiol.*, **68**, 184 (2000).
16. L. Cursino, S.V.M. Mattos, V. Azevedo, F. Galarza, D.H. Bucker, E. Chartone-Souzaa and A.M.A. Nascimento, *Sci. Total. Environ.*, **261**, 109 (2000).
17. Z. Yassin, E. Ortiz-Salmeron, F. Garcia-Maroto, C. Baron and L. Garcia-Fuentes, *Biochim. Biophys. Acta*, **1698**, 227 (2004).
18. T.H. Rushmore and C.B. Pickett, *J. Biol. Chem.*, **268**, 11475 (1993).
19. M.A. McTigue, D.R. Williams and J.A. Tainer, *J. Mol. Biol.*, **246**, 21 (1995).
20. S.C. Gill and P.H. von Hippel, *Anal. Biochem.*, **182**, 319 (1989).
21. M.R. Eftink and C.A. Ghiron, *Anal. Biochem.*, **114**, 199 (1981).
22. J.R. Lakowicz. Principles of Fluorescence Spectroscopy, edn. 2, pp. 13-120 (1999).
23. R. Narazaki, T. Maruyama and M. Otagiri, *Biochim. Biophys. Acta*, **1338**, 275 (1997).
24. L. Rulíšek and J.Vondrášek, *J. Inorg. Biochem.*, **71**, 115 (1998).
25. K. Lim, J.X. Ho, K. Keeling, G.L. Gilliland, X. Ji, F. Rüker and D.C. Carter, *Protein Sci.*, **3**, 2233 (1994).
26. E.H. Strickland, *CRC Crit. Rev. Biochem.*, **2**, 113 (1974).

(*Received*: 21 May 2009; *Accepted*: 14 January 2010) AJC-8294